Cellular/Molecular

KCNQ/M Channels Control Spike Afterdepolarization and Burst Generation in Hippocampal Neurons

Cuiyong Yue and Yoel Yaari
Department of Physiology, Institute of Medical Sciences, Hebrew University–Hadassah Faculty of Medicine, Jerusalem 91120, Israel

KCNQ channel subunits are widely expressed in peripheral and central neurons, where they give rise to a muscarinic-sensitive, subthreshold, and noninactivating K^+ current (M-current). It is generally agreed that activation of KCNQ/M channels contributes to spike frequency adaptation during sustained depolarizations but is too slow to influence the repolarization of solitary spikes. This concept, however, is based mainly on experiments with muscarinic agonists, the multiple effects on membrane conductances of which may overshadow the distinctive effects of KCNQ/M channel block. Here, we have used selective modulators of KCNQ/M channels to investigate their role in spike electrogenesis in CA1 pyramidal cells. Solitary spikes were evoked by brief depolarizing current pulses injected into the neurons. The KCNQ/M channel blockers linopirdine and XE991 markedly enhanced the spike afterdepolarization (ADP) and, in most neurons, converted solitary ("simple") spikes to high-frequency bursts of three to seven spikes ("complex" spikes). Conversely, the KCNQ/M channel opener retigabine reduced the spike ADP and induced regular firing in bursting neurons. Selective block of BK or SK channels had no effect on the spike ADP or firing mode in these neurons. We conclude that KCNQ/M channels activate during the spike ADP and limit its duration, thereby precluding its escalation to a burst. Consequently, down-modulation of KCNQ/M channels converts the neuronal firing pattern from simple to complex spiking, whereas up-modulation of these channels exerts the opposite effect.

Key words: **hippocampus; KCNQ; M current; afterdepolarization; bursting; pyramidal cell**

Introduction

The M-type K^+ current (M current or I_M) originally discovered in sympathetic neurons (Brown and Adams, 1980) is ubiquitous in the nervous system. It is a slow, low-voltage-activating, noninactivating K^+ current that is suppressed by muscarinic agonists. Many other neurotransmitters converge to either upregulate or downregulate I_M via a variety of second messenger cascades (Brown and Yu, 2000). Recent evidence suggests that native neuronal M channels are formed by heteromeric assemblies of KCNQ subunits, particularly KCNQ2, KCNQ3, and KCNQ5 (Brown and Yu, 2000). When these channel subunits are coexpressed in *Xenopus* oocytes, a K^+ current is displayed that shares many characteristics with I_M, including voltage dependence, kinetics, and pharmacology (Wang et al., 1998; Schroeder et al., 2000).

What is the physiological function of I_M? Because the activation time constant of I_M is in the order of tens of milliseconds, it is generally agreed that it cannot contribute significantly to the repolarization of fast action potentials (Storm, 1987, 1989). Yet, I_M activation during sustained depolarizations will tend to hyperpolarize the neuron and reduce its firing rate. Hence, I_M is thought to contribute to the phenomenon of spike frequency adaptation that is seen in numerous peripheral and central neurons (Brown, 1988). This hypothesis is supported by studies showing that muscarinic agonists markedly reduce spike frequency adaptation (Cole and Nicoll, 1983; Madison and Nicoll, 1984; McCormick et al., 1993). It should be noted, however, that muscarinic excitation modulates not only M channels but also many other types of channels (Caulfield et al., 1993). Hence, the unique function of I_M cannot be reliably ascertained by the use of muscarinic agonists.

Several drugs that selectively modulate both heterologously expressed and native KCNQ/M channels have been discovered in recent years (Brown and Yu, 2000). The "cognition enhancers" linopirdine and XE991 were shown to block I_M (Aiken et al., 1995; Schnee and Brown, 1998; Wang et al., 1998), whereas the anticonvulsant drug retigabine was found to increase I_M (Rundfeldt and Netzer, 2000; Wickenden et al., 2000; Tatulian et al., 2001). The availability of these drugs now permits a more precise examination of the functional roles of native KCNQ/M channels in normal and pathological conditions (Hu et al., 2002; Passmore et al., 2003). Using these drugs to modulate I_M in hippocampal pyramidal cells, we show here that this current controls the intrinsic firing pattern of these neurons. Through this previously unexpected action of I_M, KCNQ/M channels may determine the input–output relationships of neurons in the nervous system.

Materials and Methods

Slice preparation. All experimental protocols were approved by the Hebrew University Animal Care and Use Committee. Transverse hippocampal slices were prepared from adult Sabra rats (150–200 gm). Animals were anesthetized with ether or isoflurane (3–4%) and decapi-

Received Dec. 6, 2003; revised April 7, 2004; accepted April 7, 2004.

This work was supported by the German–Israel collaborative research program of the Bundesministerium für Bildung und Forschung and the Ministry of Science, the Deutsche Forschungsgemeinschaft (SFB TR3), the Niedersachsen Foundation, and the Henri J. and Erna D. Leir Chair for Research in Neurodegenerative Diseases.

Correspondence should be addressed to Dr. Yoel Yaari, Department of Physiology, Hebrew University School of Medicine, P.O. Box 12272, Jerusalem 91121, Israel. E-mail: yaari@md.huji.ac.il.

DOI:10.1523/JNEUROSCI.0765-04.2004

 0270-6474/04/244614-11$15.00/0

Table 1. Effects of KCNQ/M channel modulators linopirdine (10 μM), XE991 (3 μM), and retigabine (10 μM) on passive and active membrane properties of CA1 pyramidal cells

	Control ($n = 20$)	Linopirdine ($n = 20$)	Control ($n = 7$)	XE991 ($n = 7$)	Control ($n = 5$)	Retigabine ($n = 5$)
Resting potential (mV)	−69.9 ± 3.3*	−64.7 ± 4.8*	−67.7 ± 3.2	−65.6 ± 3.2	−68.0 ± 2.1*	−72.8 ± 3.2*
Input resistance (MΩ)	35.4 ± 11.7*	40.3 ± 16.6*	38.9 ± 11.6	44.7 ± 16.1	40.1 ± 11.3*	24.8 ± 3.1*
Spike threshold (mV)	−58.9 ± 2.8	−56.9 ± 3.9	−62.5 ± 5.1	−61.8 ± 4.4	−63.5 ± 3.8	−60.2 ± 4.8
Spike rise time (msec)	0.16 ± 0.49	0.14 ± 0.3	0.15 ± 0.4	0.14 ± 0.24	0.14 ± 0.23	0.15 ± 0.25
Spike amplitude (mV)	92.0 ± 7.0	93.6 ± 6.6	96.6 ± 6.7	97.9 ± 7.5	96.6 ± 5.5	98.1 ± 3.6
Spike width (msec)	0.83 ± 0.09*	0.95 ± 0.17*	0.84 ± 0.62*	0.90 ± 0.3*	0.85 ± 0.1*	0.97 ± 0.1*
Fast AHP (msec)	−60.1 ± 3.3*	−57.7 ± 3.4*	−61.9 ± 4.9*	−60.2 ± 4.5*	−62.4 ± 2.6	−59.4 ± 3.5
ADP size (mV·msec)	180.3 ± 40.1*	295.2 ± 89.9*	180.9 ± 77.8*	287.6 ± 109.8*	203.5 ± 58.2*	132.2 ± 61.3*

The asterisks denote significant differences between mean values in controls versus the drug-treated group (paired Student's *t* test; $p < 0.05$).

tated with a guillotine. The brain was removed and immersed immediately in ice-cold oxygenated (95% O_2–5% CO_2) dissection artificial CSF (ACSF). The caudal two-thirds of one hemisphere (containing one hippocampus) were glued to the stage of a vibratome (Leica, Nussloch, Germany). Transverse slices (400 μm thick) were cut from the region of the hemisphere containing the anterior hippocampus. The hippocampal portion was dissected out of each slice, and the CA3 region was removed. The slices were transferred to an incubation chamber containing oxygenated saline at room temperature (21–24°C), where they were allowed to recover at least 1 hr. The slices were transferred one at a time to an interface slice chamber and perfused from below with oxygenated (95% O_2–5% CO_2) ACSF at 33.5°C. The upper surface of the slices was exposed to the humidified gas mixture.

The standard ACSF contained (in mM) 124 NaCl, 3.5 KCl, 2 $MgSO_4$, 1.6 $CaCl_2$, 26 $NaHCO_3$, and 10 D-glucose, pH 7.3. To obtain high K^+-ACSF, the KCl concentration was raised to 7.5 mM. To obtain Ca^{2+}-free ACSF, the $CaCl_2$ was replaced with equimolar $MgCl_2$. In most experiments, the ACSFs also contained the glutamate receptor antagonists CNQX (15 μM) and APV (50 μM) to block fast EPSPs and the $GABA_A$ receptor antagonist picrotoxin (100 μM) to block fast IPSPs. Other drugs were added to the ACSF as indicated.

Electrophysiological methods. Current-clamp recordings from the somata of pyramidal cells in the CA1 pyramidal layer were made using sharp, K^+-acetate-filled (4 M) glass microelectrodes (70–100 MΩ). An active bridge circuit in the amplifier (Axoclamp 2A; Axon Instruments, Foster City, CA) allowed simultaneous injection of current and measurement of membrane potential. The bridge balance was carefully monitored and adjusted before each measurement. The pyramidal cells accepted for this study had stable resting potentials of at least −60 mV and overshooting action potentials.

Chemicals. All chemicals and drugs were purchased from Sigma Chemicals (Petach-Tikva, Israel), except for CNQX (Research Biochemicals, Natick, MA), apamin and iberiotoxin (Alomone Labs, Tel-Aviv, Israel), and retigabine and XE991 (a kind gift from Dr. J. B. Jensen, Neurosearch, Copenhagen, Denmark). Stock solutions (10 mM) of linopirdine (in ethanol), XE991, and retigabine (in dimethylsulfoxide) were stored at −20°C. Ethanol and DMSO added to the standard ACSF to a concentration of 0.001% had no effects on the measured spike parameters.

Data measurement and analysis. The intracellular signals were digitized, stored, and analyzed using a Pentium computer and the pCLAMP9 data acquisition system (Axon Instruments). Apparent input resistance was measured from voltage deflections induced by small (50–100 pA) 200 msec negative current pulses. Spike rise time was measured from spike onset to peak. Spike width was measured at 50% of spike amplitude. The size of the spike afterdepolarization (ADP) was measured as the integrated "area under the curve" between the fast afterhyperpolarization (fAHP) and the point at which membrane voltage returned to resting potential. The intraburst firing rates were calculated from the mean interspike interval. Averaged data are expressed as means ± SD. The significance of the differences between the measured spike parameters was evaluated using Student's paired *t* test with a significance level ≤0.05.

Results

The KCNQ/M channel blocker linopirdine induces intrinsic bursting by augmenting the spike ADP

To explore the function of KCNQ/M channels in shaping the intrinsic firing pattern of principal brain neurons, we examined the effects of selective KCNQ/M channel modulators on spike electrogenesis in CA1 pyramidal cells. Previous studies have confirmed that these neurons express KCNQ/M channels (Shah et al., 2002) that give rise to a conspicuous I_M on depolarization (Halliwell and Adams, 1982; Aiken et al., 1995; Schnee and Brown, 1998; Schweitzer, 2000). To isolate the drug effects on intrinsic membrane properties, fast synaptic excitation and inhibition were blocked pharmacologically in most experiments.

We first examined the effects of the KCNQ/M channel blocker linopirdine. This drug blocks I_M in CA1 pyramidal cells with reported IC_{50} values ranging from 2.4 to 8.5 μM (Aikin et al., 1995; Schnee et al., 1998; Shah et al., 2002). We routinely used a concentration of 10 μM linopirdine that inhibits 75–90% of I_M in hippocampal neurons. At this concentration, linopirdine exerts only small effects, if at all, on other slow K^+ currents (see below) and has no detectable effects on persistent Na^+ current (I_{NaP}) in CA1 hippocampal cells (D. Sochivko, V. Belzer, and Y. Yaari, unpublished observations). Adding 10 μM to the ACSF depolarized the neurons by 2–10 mV (mean, 5.1 ± 2.5; $n = 20$) (Table 1). Action potentials were evoked by injecting the neurons with threshold-straddling, brief (4 msec) and long (180 msec) depolarizing current pulses through the recording microelectrode. Linopirdine exerted several effects on active membrane properties (Table 1). The most conspicuous effect was facilitation of the spike ADP. In adult CA1 pyramidal cells, the fast repolarization of the somatic action potential is incomplete, and the depolarization state is maintained for tens of milliseconds, much longer than would be expected from passive recharging of the somatic membrane (Schwartzkroin, 1975; Jensen et al., 1996). This is attributable primarily to the activation of I_{NaP} (Azouz et al., 1996; Su et al., 2001). As illustrated in Figure 1*A*, concurrently with depolarizing the neuron by 4 mV (from −70 to −66 mV), switching to ACSF containing 10 μM linopirdine caused progressive augmentation of ADP amplitude and slowing of its decay, ultimately converting the single spike response to a burst of three spikes (Fig. 1*Aa*$_1$–*a*$_3$,*B*). With time, bursting activity also appeared spontaneously despite the blockage of synaptic excitation, attaining a rhythm of ~0.8 Hz (Fig. 1*Aa*$_4$). The effects of linopirdine were reversible on 30–40 min of drug washout ($n = 4$).

In a series of 60 CA1 pyramidal cells treated with 10 μM linopirdine, the spike ADP was facilitated in all cases, and 49 of these neurons (82%) converted to the burst mode within 30–40

min of exposure to the drug. The number of spikes within bursts evoked by brief stimuli was consistent for each neuron and varied between three and seven (mean, 4.8 ± 1.2; $n = 30$) across neurons. The spike frequency within bursts was also consistent for each neuron and varied across neurons between 121.9–259.6 Hz (mean, 185.5 ± 38.5; $n = 30$).

Depolarization of CA1 pyramidal cells does not ordinarily induce bursting activity (Jensen et al., 1994, 1996). Hence, the induction of intrinsic bursting by linopirdine is not simply a consequence of its depolarizing effect. Indeed, in 9 of the 60 neurons in this series, linopirdine caused a marked enhancement of the ADP and induced bursting before any depolarization. Likewise, linopirdine also exerted these effects when the neurons were repolarized with steady negative current injection to their native resting potential (Fig. 1*Ab*$_1$–*b*$_4$,*C*). However, spontaneous, rhythmic bursting was less likely to occur in this condition. When the neurons were stimulated with long depolarizing current pulses, the tendency for spike clustering appeared early during the exposure to linopirdine and developed into a full burst in parallel with the growth of the spike ADP (Fig. 1*Ac*$_1$–*c*$_4$) (the minimal response to long depolarizing stimuli gradually increases from one to four spikes).

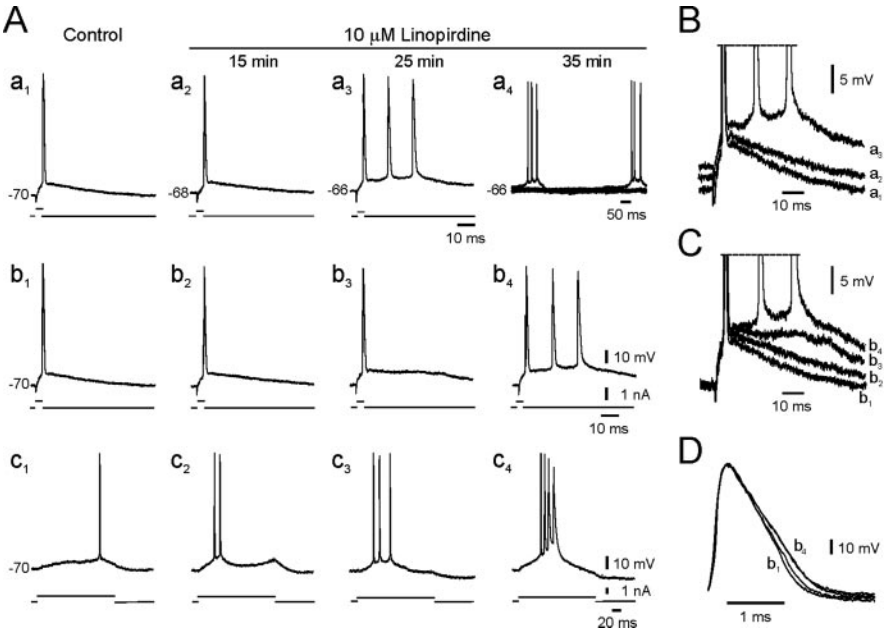

Figure 1. Effects of linopirdine on the spike ADP and firing pattern in a CA1 pyramidal cell. *A*, Intracellular recordings of the spikes evoked by brief (4 msec) and long (180 msec) threshold-straddling depolarizing current pulses. In each panel, the current stimulus is depicted below the voltage trace. Resting potential (in millivolts) is shown to the left of the voltage trace. In control, the neuron fired a solitary spike in response to a brief stimulus (a_1). Adding 10 μM linopirdine to the ACSF caused a gradual depolarization of the neuron (from −70 to −66 mV) and facilitation of the spike ADP (a_2, a_3), ultimately converting regular firing to spontaneous bursting (a_4; three superimposed traces). The ADP facilitation also occurred when membrane potential was maintained at its native value (−70 mV) by injecting steady negative current (b_1–b_4). Spike clustering was seen early during exposure to linopirdine when the neuron was stimulated with long depolarizing current pulses (c_1–c_4). *B*, Overlay of expanded portions of the voltage traces a_1–a_3, showing the facilitation of the spike ADP by linopirdine. *C*, Overlay of expanded portions of the voltage traces b_1–b_4, showing that even when membrane potential was maintained constant, linopirdine decreased the fAHP and augmented the spike ADP. *D*, Overlay of expanded portions of the voltage traces b_1–b_4, showing that linopirdine caused slowing of spike repolarization without affecting the rising phase of the spike.

We also tested the effects of lower linopirdine concentrations (0.1–3 μM) on the spike ADP. As shown in Figure 2, linopirdine consistently caused an increase in ADP size in a dose-dependent manner. The lowest concentration to cause a detectable increase in ADP size was 0.3 μM linopirdine (a concentration that blocks <10% of I_M in CA1 pyramidal cells) (Schnee and Brown, 1998; Shah et al., 2002). Increasing the concentration of linopirdine caused additional growth of the ADP (Fig. 2*Aa*$_1$–*a*$_5$,*B*). The cumulative data from these experiments are summarized in Figure 2*C*. When the resting membrane potential was maintained at its native value, exposing the neurons to 0.3, 1, 3, and 10 μM linopirdine facilitated the ADP by 11 ± 9.9% ($n = 9$), 32.5 ± 18.8% ($n = 10$), 59.1 ± 32.4% ($n = 10$), and 64.3 ± 39.9% ($n = 20$), respectively. It should be noted, however, that once a neuron converted to the bursting mode, its ADP could not be measured. Therefore, the spike ADPs in 3 and 10 μM linopirdine are probably underestimated, because linopirdine at these concentrations induced bursting in 42.8 and 82.0% of the neurons, respectively. Although 1 μM linopirdine (a concentration that blocks ~15% of I_M) (Schnee and Brown, 1998; Shah et al., 2002) did not produce overt bursting behavior, many neurons exposed to this dose generated bursts at the onset of long depolarizing current pulses (Fig. 2*Ab*$_3$).

Other effects of linopirdine on the spike waveform

In addition to modestly depolarizing the neurons and markedly enhancing the spike ADP, several other effects of linopirdine (0.1–10 μM) on passive and active membrane properties of CA1 pyramidal cells were noted. These effects were quantified at the native (control) resting potential using negative current injection to counteract the depolarizing action of linopirdine. Linopirdine caused a small (13.8%), but significant, increase in apparent input resistance (Table 1), suggesting that some KCNQ/M channels are open even at resting potential. It did not significantly affect spike threshold, rise time, or amplitude (Table 1). However, in many neurons, linopirdine also modified the down stroke (i.e., the fast repolarization phase) of the spike. As illustrated in Figure 1*D*, this action was manifested as a modest slowing of repolarization, particularly its latter part, and as a reduction in the over all magnitude of repolarization. We quantified these effects by measuring linopirdine-induced changes in spike width and in the fAHP (i.e., the notch marking the end of the fast repolarization phase and the beginning of the ADP) (Storm, 1987). In the representative experiment shown in Figure 1, linopirdine increased spike width by 12.3% and reduced the fAHP by 3 mV. On average, 10 μM linopirdine caused spike broadening by 13.8 ± 12.5% and reduced the fAHP by 3.1 ± 2.5 mV ($n = 20$) (Table 1). At lower doses of linopirdine (0.3–3 μM), these effects were smaller and much more variable.

Neither the increases in spike width nor the decreases in fAHP showed a significant correlation with the associated increases in spike ADP. Indeed, in some neurons, spike width was virtually unaffected by linopirdine, although the ADP was markedly enhanced. Likewise, the appearance of bursting in linopirdine-treated neurons was also independent of the changes in spike repolarization. Thus, spike widths and fast AHPs in neurons that changed to bursting mode (0.81 ± 0.12 msec and −55.0 ± 5.7

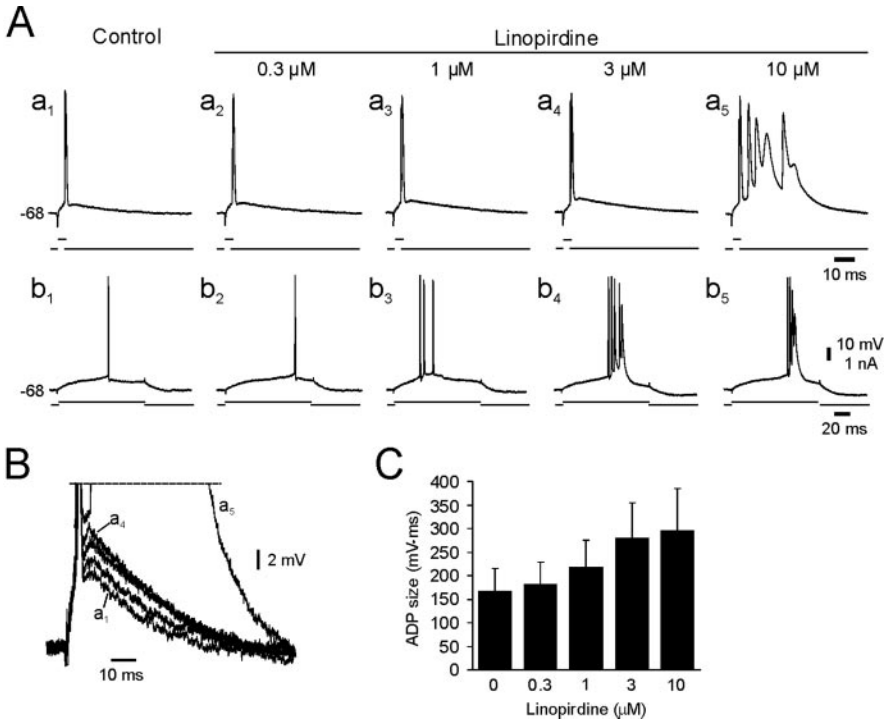

Figure 2. Effects of different doses of linopirdine on the spike ADP and firing pattern in a CA1 pyramidal cell. *A*, Intracellular recordings of the spikes evoked by brief (a_1–a_5) and long (b_1–b_5) threshold-straddling depolarizing current pulses. In control, the neuron fired a solitary spike in response to these stimuli. Exposing the neuron to increasing concentrations of linopirdine (0.3, 1, 3, and 10 μM; exposure to each concentration lasted 30 min) caused a dose-dependent increase in the spike ADP and the propensity to burst fire. The resting potential was maintained at its native value (−68 mV) by injecting steady negative current. *B*, Overlay of expanded portions of the voltage traces a_1–a_5, showing that linopirdine decreased the fAHP and augmented the ADP in a dose-dependent manner. *C*, Bar diagram summarizing of the effects of different concentrations of linopirdine on the spike ADP size in CA1 pyramidal cells. The numbers of neurons averaged in each condition were 30 (control; no linopirdine), 9 (0.3 μM), 10 (1 μM), 10 (3 μM), and 20 (10 μM linopirdine).

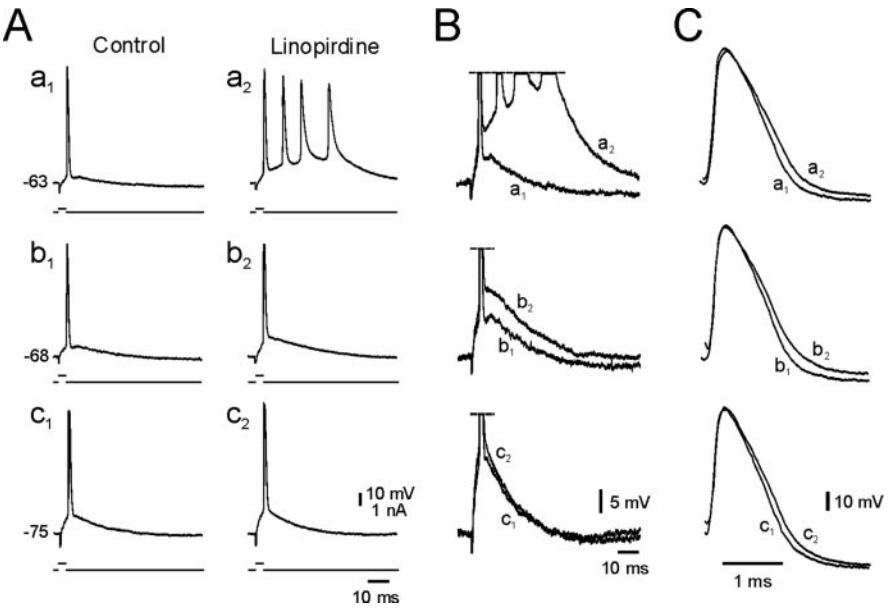

Figure 3. The facilitatory action of linopirdine on the spike ADP depends on membrane potential. *A*, Intracellular recordings of spikes evoked by brief depolarizing current pulses at resting potential (−68 mV) and at depolarized (−63 mV) and hyperpolarized (−75 mV) potentials in control ACSF (a_1, b_1, c_1) and during exposure to 3 μM linopirdine (a_2, b_2, c_2). *B*, Overlay of expanded portions of the voltage traces in *A*, showing that linopirdine facilitated the spike ADP at resting potential (b_1, b_2). This effect was enhanced by depolarization (a_1, a_2) and abolished by hyperpolarization (c_1, c_2). *C*, Overlay of expanded portions of the voltage traces in *A*, showing that a modest slowing of spike repolarization after linopirdine exposure is apparent at the three membrane potentials examined.

mV; $n = 20$) were similar to those that did not (0.86 ± 0.08 msec and −56.2 ± 5.6 mV; $n = 10$; differences not significant). In contrast, the spike ADPs in bursting neurons, measured just before the appearance of bursting (335.9 ± 73.6 mV·msec; $n = 20$), were significantly larger than in nonbursting neurons (213.9 ± 59.6 mV·msec; $n = 10$). These data suggest that the linopirdine-induced ADP facilitation underlies the appearance of intrinsic bursting, but this effect is not causally related to the attenuation of fast spike repolarization.

Voltage dependence of linopirdine effects

We also examined in five neurons how changes in resting membrane potential affect the various actions of linopirdine on the spike waveform. The neurons were depolarized and hyperpolarized from their native resting potential by steady current injection. A representative experiment is shown in Figure 3. Exposing the neuron to 3 μM linopirdine, while maintaining its native resting potential (−68 mV) with negative current injection, markedly enhanced the spike ADP (Fig. 3*A*, Bb_1,b_2). This effect was greatly amplified by depolarizing the neuron to −63 mV, causing the ADP to trigger a burst (Fig. 3*A*, Ba_1,b_2). Conversely, when the neuron was hyperpolarized to −75 mV, there was practically no change in the ADP after linopirdine treatment (Fig. 3*A*, Bc_1,c_2). Yet, linopirdine caused spike broadening and fAHP decrease at all three membrane potentials (Fig. 3*C*). Similar results were obtained in all five neurons. These data suggest that linopirdine affects the spike ADP and spike repolarization through disparate mechanisms.

The KCNQ/M channel blocker XE991 mimics the effects of linopirdine

The cognition enhancer XE991 is reportedly even more effective than linopirdine in blocking heteromeric KCNQ2+3 channels and neuronal I_M (IC_{50}, ~1 μM) (Wang et al., 1998). Therefore, we also tested how this drug affects intrinsic neuronal firing patterns. A representative experiment is illustrated in Figure 4. At a concentration of 3 μM (expected to block ~80% of I_M) (Wang et al., 1998), XE991 mimicked the effects of 10 μM linopirdine in modestly depolarizing the neuron by 4 mV (from −72 to −68 mV). On average, 3 μM XE991 depolarized the neurons by 2.1 ± 1.7 mV ($n = 7$) (Table 1). Concurrently, XE991 enhanced the spike ADP until it elicited a burst (Fig. 4Aa_1–a_3,*B*). With time, the neuron developed rhythmic

bursting (Fig. 4*Aa*$_4$). Again, XE991 facilitated the spike ADP also when the native resting potential was maintained by steady negative current injection (Fig. 4*Ab*$_1$–*b*$_4$,*C*). In seven experiments, 3 μM XE991 caused, on average, a 69.1% increase in ADP size (Table 1) and converted four of these neurons (57.1%) into the bursting mode at the native resting potential. When neurons exposed to XE991 were stimulated with long depolarizing current pulses, they displayed a tendency for spike clustering even when brief stimuli evoked one spike only (Fig. 4*Ac*$_1$–*c*$_4$). We also tested in six neurons the action of 1 μM XE991 (expected to block ~50% of I_M) (Wang et al., 1998). In these neurons, XE991 caused a 47.3 ± 48.0% increase in ADP size and converted two of them (33.3%) to bursting mode.

When measured from the native resting potential, XE991 (3 μM), like linopirdine, caused a modest (14.9%) increase in apparent input resistance (although this change did not attain statistical significance) (Table 1). It did not affect spike threshold, rise time, or amplitude (Table 1). Also, like linopirdine, it attenuated the fast repolarization phase of the spike (Fig. 4*D*). In seven neurons, XE991 caused spike broadening by 7.9 ± 5.1% and reduced the fAHP by 1.7 ± 0.8 mV, respectively (Table 1). The effects of XE991 were reversible on 30–40 min of drug washout ($n = 2$).

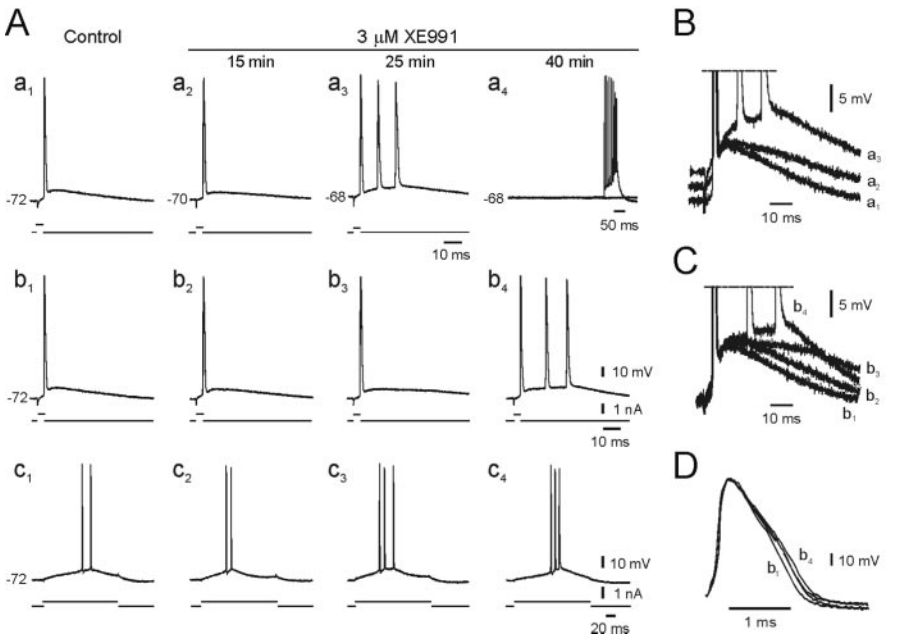

Figure 4. Effects of XE991 on the spike ADP and firing pattern in a CA1 pyramidal cell. *A*, Intracellular recordings of the spikes evoked by brief and long threshold-straddling depolarizing current pulses. In control, the neuron fired a solitary spike in response to brief stimuli (a_1). Adding 3 μM XE991 to the ACSF caused a gradual depolarization of the neuron (from −72 to −68 mV) and facilitation of the spike ADP (a_1–a_3), ultimately converting regular firing to spontaneous bursting (a_4; two superimposed traces). The ADP facilitation also occurred when membrane potential was maintained at its native value (−72 mV) by injecting steady negative current (b_1–b_4). Spike clustering was seen early during exposure to linopirdine when the neuron was stimulated with long depolarizing current pulses (c_1–c_4). *B*, Overlay of expanded portions of the voltage traces a_1–a_3, showing the facilitation of the spike ADP by XE991. *C*, Overlay of expanded portions of the voltage traces b_1–b_4, showing that even when membrane potential was maintained constant, XE991 augmented the spike ADP. *D*, Overlay of expanded portions of the voltage traces b_1–b_4, showing that XE991 caused modest slowing of spike repolarization without affecting the rising phase of the spike.

Effects of blockers of other K^+ currents on the spike waveform

In CA1 pyramidal cells, the big conductance Ca^{2+}-activated K^+ (BK) current, I_C, is responsible for the late phase of spike repolarization; blocking I_C causes spike broadening and decreases the fAHP (Lancaster and Nicoll, 1987; Storm, 1987). Moreover, I_C also has been implicated, conjointly with I_M, in the generation of a medium AHP (mAHP; duration, 20–40 msec) that normally is seen after a short train of action potentials (Storm, 1989). It has been reported that, in addition to blocking I_M, linopirdine also blocks I_C, albeit with a sevenfold lower affinity compared with the blockage of I_M (IC_{50} values, 16.3 vs 2.4 μM) (Schnee and Brown, 1998). Nonetheless, even a small reduction of I_C may contribute to some of the observed effects of linopirdine. Therefore, we investigated how blocking I_C with selective antagonists mimics and interacts with the actions of linopirdine.

We used paxilline and iberiotoxin, selective and potent blockers of BK channels (Shao et al., 1999), to examine the effects of inhibiting I_C on the spike waveform. Representative experiments with paxilline (10 μM; $n = 7$) and iberiotoxin (100 nM; $n = 7$) are shown in Figure 5. Expectedly, both paxilline and iberiotoxin caused marked broadening of the spike (by 30.5 ± 30.7% and 25.3 ± 20.3%, respectively) and significantly decreased the fAHP (by 6.1 ± 3.9 mV and 4.1 ± 2.1 mV, respectively) (Fig. 5*A*,*B*, bottom). However, neither paxilline nor iberiotoxin significantly affected the spike ADP or modified the regular firing pattern of the treated neurons (Fig. 5*A*,*B*, top). Notwithstanding, exposing paxilline-treated ($n = 4$) or iberiotoxin-treated ($n = 3$) neurons to 10 μM linopirdine resulted in spike ADP augmentation and the appearance of bursting (Fig. 5*A*,*B*, dashed traces in top panels). In contrast, linopirdine had almost no effect on spike repolarization in these neurons (Fig. 5*A*,*B*, bottom). These data suggest that blocking I_C selectively occludes the effects of linopirdine on spike repolarization but not on the spike ADP.

Recent data suggest that in CA1 pyramidal cells, activation of small conductance Ca^{2+}-activated K^+ (SK) channels during repetitive firing (giving rise to a K^+ current designated I_{AHP}), may also contribute to the generation of the mAHP (Stocker et al., 1999). These channels are blocked by apamin and methyl derivatives of bicuculline (Khawaled et al., 1999; Stocker et al., 1999). Although SK channels are resistant to linopirdine (Dreixler et al., 2000), we were interested to know whether they regulate the spike ADP. Therefore, we examined the effects of apamin and bicuculline methiodide on this afterpotential. In five experiments, adding 50 nM apamin to the ACSF did not significantly modify spike width or the fAHP (Fig. 5*C*, bottom). Likewise, apamin had no significant effect on the spike ADP (Fig. 5*C*, top). Exposing apamin-treated neurons to 10 μM linopirdine ($n = 4$) caused spike broadening and fAHP decrease (Fig. 5*C*, bottom) and also caused ADP facilitation and the appearance of bursting (Fig. 5*C*, top). Interestingly, although it had no effects of its own, pretreatment with apamin markedly enhanced the facilitatory effect of linopirdine, resulting in bursts of 10 spikes or more.

Surprisingly, adding 10 μM bicuculline methiodide to the ACSF ($n = 5$) caused significant spike broadening (by 25.2 ± 9.2%) and reduced the fAHP (by 3.3 ± 3.1 mV) (Fig. 5*D*, bottom), suggesting that this drug may also block K^+ conductances that contribute to fast spike repolarization. Bicuculline also mod-

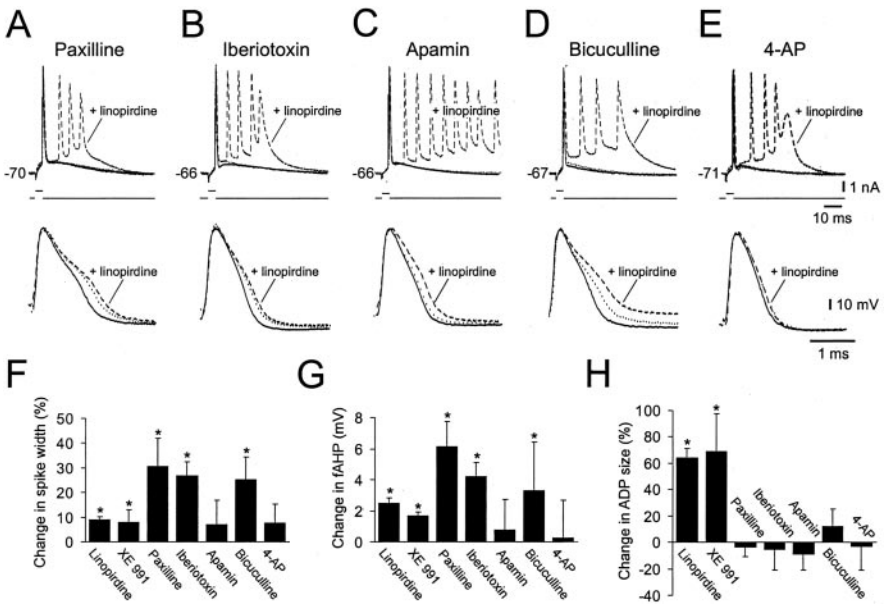

Figure 5. Comparison of the effects of blockers of different K^+ channels on spike waveform in CA1 pyramidal cells. *A*, Effects of paxilline. Top, Overlay of intracellular recordings of spikes evoked in control ASCF (solid line), 30 min after adding 10 μM paxilline (dotted line) and 20 min after adding 10 μM linopirdine to the paxilline-containing ACSF (dashed line). Paxilline had no detectible effect on the spike ADP, whereas linopirdine enhanced the ADP to the point of bursting. Bottom, Data are the same as above, but at an expanded time scale, showing spike broadening by paxilline. *B*, Effects of iberiotoxin. Recordings from another neuron in control ASCF (solid line), 30 min after adding 100 nM iberiotoxin to the ACSF (dotted line) and 25 min after adding 10 μM linopirdine to the iberiotoxin-containing ACSF (dashed line). Iberiotoxin blocked the fAHP but had no visible effect on the spike ADP, whereas linopirdine enhanced the ADP to the point of bursting. Bottom, Expanded traces showing attenuation of spike repolarization by iberiotoxin. *C*, Effects of apamin. Recordings from another neuron in control ASCF (solid line), 30 min after adding 50 nM apamin to the ACSF (dotted line) and 30 min after adding 10 μM linopirdine to the apamin-containing ACSF (dashed line). Apamin did not affect the spike ADP, whereas linopirdine induced an intense burst response. Bottom, Expanded traces showing that apamin does not affect spike repolarization. *D*, Effects of bicuculline. Recordings from another neuron in control ASCF (solid line), 30 min after adding 10 μM bicuculline methiodide to the ACSF (dotted line) and 30 min after adding 10 μM linopirdine to the bicuculline-containing ACSF (dashed line). Bicuculline slightly augmented the spike ADP, whereas linopirdine facilitated it to the point of bursting. Bottom, Expanded traces showing that bicuculline markedly attenuates spike repolarization, and this effect was further enhanced by linopirdine. *E*, Effects of 4-AP. Recordings from another neuron in control ASCF (solid line), 30 min after adding 100 μM 4-AP to the ACSF (dotted line) and 20 min after adding 10 μM linopirdine to the 4-AP-containing ACSF (dashed line). The spike ADP was not affected by 4-AP, whereas linopirdine induced a burst response. Bottom, Expanded traces showing that no effect of 4-AP on fast spike repolarization. *F–G*, Bar diagrams summarizing the effects of the seven K^+ channel blockers on spike width (expressed as percentage of control), fAHP (expressed as absolute change in millivolts), and spike ADP size (expressed as percentage of control), respectively. Each bar represents the change in spike parameter after 30 min of exposure to a drug. The number of neurons in each of the five experimental groups was 20 (linopirdine), 7 (XE991), 7 (paxilline), 7 (iberiotoxin), 5 (apamin), 5 (bicuculline), and 6 (4-AP). The asterisks above the bars denote that the observed changes were statistically significant.

estly enhanced the spike ADP (11.8 ± 13.3%) (Fig. 5*D*, top), but this effect was not statistically significant. Exposing bicuculline-treated neurons ($n = 4$) to 10 μM linopirdine caused additional spike broadening and fAHP decrease (Fig. 5*D*, bottom) and also caused ADP facilitation and the appearance of bursting (Fig. 5*D*, top).

To complete the search for K^+ currents involved in shaping the spike ADP, we investigated the contribution of the low-voltage-activating, slowly inactivating D-type K^+ current (I_D), which is blocked by low concentrations of 4-AP (Storm, 1988). We tested the effects of 100 μM 4-AP on the spike waveform in six neurons. We found no significant changes in spike width, fAHP, and spike ADP, yet the addition of 10 μM linopirdine ($n = 4$) caused spike broadening and enhanced the spike ADP, inducing bursting in three of these neurons (Fig. 5*E*). The lack of a 4-AP effect on spike repolarization and ADP is not unexpected, given that >90% of I_D conductance is inactivated at a normal resting potential (Storm, 1988).

Figure 5, *F–H*, provides a summary of the effects of linopirdine, XE991, paxilline, iberiotoxin, apamin, bicuculline, and 4-AP on the spike waveform in CA1 pyramidal cells. Most of these drugs attenuated fast spike repolarization, with paxilline and iberiotoxin exerting the largest effects. Of all these drugs, however, only linopirdine and XE991 strongly facilitated the spike ADP (Fig. 5*H*). Cumulatively, these results suggest that I_C, I_{AHP}, and I_D do not significantly regulate the spike ADP in these neurons, whereas I_M plays a critical role in reducing this afterpotential.

Effects of the KCNQ/M channel opener retigabine on the spike waveform

Retigabine has been shown to increase heteromeric KCNQ/M channel current by shifting its voltage dependence of activation to one more hyperpolarized, as well by increasing its rate of activation and slowing its rate of deactivation (Main et al., 2000; Wickenden et al., 2000; Tatulian et al., 2001). If indeed, as suggested above, the spike ADP is curtailed by activation of KCNQ/M channels during the ADP, then retigabine application should reduce the spike ADP. We tested this prediction using 1, 3, and 10 μM retigabine. Adding retigabine to the ACSF mildly hyperpolarized all neurons. At a concentration of 10 μM, retigabine hyperpolarized the neurons by 4.8 ± 2.2 mV ($n = 5$) (Table 1). It also caused a large drop in apparent input resistance of these neurons (from 40.1 ± 11.3 to 24.8 ± 3.1 MΩ). To assess the effects of retigabine on the spike ADP, the membrane potential was maintained at its native resting value by injecting an appropriate steady positive current through the recording microelectrode. As shown in Figure 6, retigabine dose-dependently decreased the spike ADP, converting its latter part to a mAHP (Fig. 6Aa_1–a_4,*B*). Similar results were seen in all five experiments. The decrease in ADP size induced by 10 μM retigabine amounted to 30.7 ± 31.1% (Table 1). When the neurons were stimulated with long depolarizing current pulses, retigabine dose-dependently decreased the number of evoked spikes (Fig. 6Ab_1–b_4). Retigabine had no significant effect on spike threshold, rise time, and amplitude (Table 1). In some neurons, retigabine caused modest spike broadening and a decrease in the fAHP (Table 1; Fig. 6*C*).

Because of its depressant effect on the spike ADP in CA1 pyramidal cells, we expected that retigabine will also suppress intrinsic bursting in these neurons. We induced intrinsic bursting in three different ways, which are illustrated in Figure 7: (1) by raising the K^+ content of the ACSF from 3.5 to 7.5 mM ($n = 3$) (Jensen et al., 1994) (Fig. 7Aa_1,a_2); (2) by deleting Ca^{2+} ions from the ACSF ($n = 4$) (Su et al., 2001) (Fig. 7Ba_1,a_2); (3) by adding 10 μM linopirdine to the ACSF ($n = 6$) (Fig. 7Ca_1,a_2). In all these cases, adding 10 μM retigabine suppressed the burst responses by depressing their underlying spike ADP (Fig. 7Aa_3,a_4,Ba_3,a_4,Ca_3,a_4). Inter-

estingly, retigabine reversed the facilitatory effect of linopirdine on the spike ADP but not its effects on spike width and the fAHP ($n = 4$; data not shown), supporting our contention that the latter effects are not attributable to KCNQ/M channel block.

Effects of KCNQ/M channel modulators on subthreshold potentials

When CA1 pyramidal cells are stimulated repeatedly with brief, threshold-straddling depolarizing current pulses, some stimuli evoke spikes, whereas others do not. In the latter cases, the depolarized membrane potential usually repolarizes more slowly than expected from passive charging of membrane capacitance. The resultant potential transients, termed "subthreshold ADPs," may last from 40 to 100 msec. They are particularly prolonged at depolarized membrane potentials. We have previously shown that these subthreshold ADPs, like the active spike ADPs, are driven by I_{NaP} (Azouz et al., 1996; Su et al., 2001). The variation across neurons in the propensity to generate protracted subthreshold ADPs most probably reflects heterogeneity in densities of I_{NaP} and opposing outward currents.

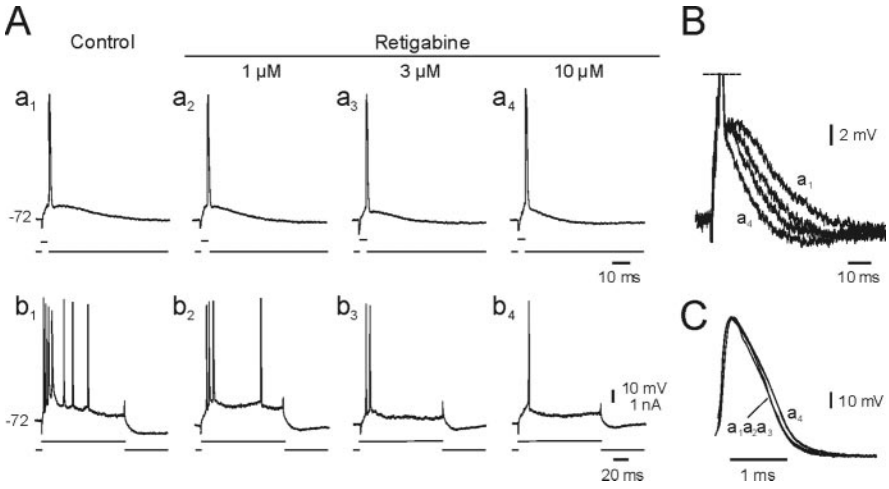

Figure 6. Effects of retigabine on the spike ADP and repetitive firing in a CA1 pyramidal cell. *A*, Intracellular recordings of the spikes evoked by brief and long depolarizing current pulses. Exposing the neuron sequentially to increasing concentrations of retigabine (1, 3, and 10 μM; exposure to each concentration lasted 30 min) hyperpolarized the neuron by 4 mV, but the resting potential was maintained at its native value (−72 mV) by injecting steady positive current. Retigabine also caused a dose-dependent decrease in the spike ADP and increase in the mAHP, without affecting the fAHP (a_1–a_4). The number of spikes elicited by long, suprathreshold depolarizing current pulses decreased as the concentration of retigabine increased (b_1–b_4). *B*, Overlay of expanded portions of the voltage traces a_1–a_4, showing that retigabine dose-dependently suppresses the spike ADP and enhances the mAHP. *C*, Overlay of expanded portions of the voltage traces a_1–a_4, showing that 10 μM retigabine slightly broadens the spike ADP.

Here, we have examined how modulating KCNQ/M channels affects the subthreshold ADPs. The effects of linopirdine are illustrated in Figure 8*A*. Two exemplary responses to brief, threshold-straddling stimuli (bottom trace), the first a spike (top trace) and the second a subthreshold response (middle trace), are shown (Fig. 8Aa_1). Adding 10 μM linopirdine to the ACSF depolarized the neuron by 4 mV, but this effect was counteracted by negative current injection. As seen in most neurons, linopirdine facilitated the spike ADP, ultimately converting the single spike to a burst (Fig. 8Aa_2, top traces). Concurrently, it also facilitated the subthreshold ADPs, converting them to slowly declining potential transients lasting 100–200 msec (Fig. 8Aa_2, middle trace). To enable comparison, the spike ADPs (Fig. 8Ab) and subthreshold ADPs (Fig. 8Ac) in control and in linopirdine have been enlarged and overlaid. It is evident that the effects of linopirdine are very similar in both cases. A similar facilitation of subthreshold ADPs by linopirdine was seen in all 12 neurons examined. They were more pronounced at depolarized membrane potentials and disappeared on hyperpolarization of the neurons. Figure 8*B* shows that XE991 (3 μM) mimicked the action of linopirdine in similarly facilitating the spike and subthreshold ADPs ($n = 5$). In contrast, exposure of the neurons to paxilline (10 μM; $n = 4$), iberiotoxin (100 nM; $n = 3$), apamin (50 nM; $n = 3$), bicuculline methiodide (10 μM; $n = 4$), and 4-AP (100 μM; $n = 3$) had no effect on the subthreshold ADPs (data not shown).

We also examined the effects of retigabine on subthreshold ADPs. These effects are shown in Figure 8*C*. Adding 10 μM retigabine to the ACSF hyperpolarized the neuron by 3 mV, but this effect was counteracted by positive current injection. As shown above, retigabine reduced the spike ADP while enhancing the following mAHP (Fig. 8a_1,a_2,b). Retigabine similarly suppressed the subthreshold ADPs, accelerating their decay and inducing a small mAHP (Fig. 8a_1,a_2,c). These effects of retigabine were seen in all six neurons examined.

Cumulatively, these data show that whenever the neuron is depolarized to near threshold potential, KCNQ/M channels are activated and impose rapid repolarization. The modulation of the spike ADP is, therefore, a particular case of a more general function of these channels (i.e., to limit the duration of any subthreshold depolarizing events).

Discussion

In this study, we investigated the functional role of KCNQ/M channels in spike electrogenesis. We show that activation of these channels normally abates the spike ADP and ensures complete repolarization of the neuron. When KCNQ/M channels are blocked, the neuron remains depolarized for a lengthy period during in which it may generate multiple spikes. Thus, KCNQ/M channels critically determine the spike output of the neuron.

KCNQ/M channel regulation of the spike ADP

In adult CA1 pyramidal cells, the active ADP component is driven primarily by I_{NaP} (Azouz et al., 1996; Su et al., 2001). This conductance activates at subthreshold membrane potentials (~−70 mV) (French et al., 1990). Therefore, a fraction of this conductance is still active at the end of spike repolarization (−55 to −60 mV). Because the Na^+ driving force is large at these potentials, a substantial I_{NaP} flows immediately after the fast spike. However, the magnitude of the resultant ADP depends not only on I_{NaP} density but also on the densities of opposing outward currents. Which of all K^+ currents operating at subthreshold potentials effectively oppose I_{NaP}? Here, we show that blocking I_M markedly enhances the spike ADP, whereas augmenting I_M exerts the opposite effect. In contrast, blocking I_C, I_{AHP}, and I_D has no significant effect on the ADP. Thus, I_M provides the major opposition to I_{NaP}. Consequently, the fate of the spike ADP depends predominantly on the ratio I_{NaP}/I_M at near threshold potentials. Decreasing this ratio by enhancing I_M or by inhibiting I_{NaP} (Alroy et al., 1999) will suppress the spike ADP and associated bursting. Conversely, increasing this ratio by blocking I_M or enhancing I_{NaP} (Su et al., 2001) will facilitate the spike ADP and induce intrinsic bursting.

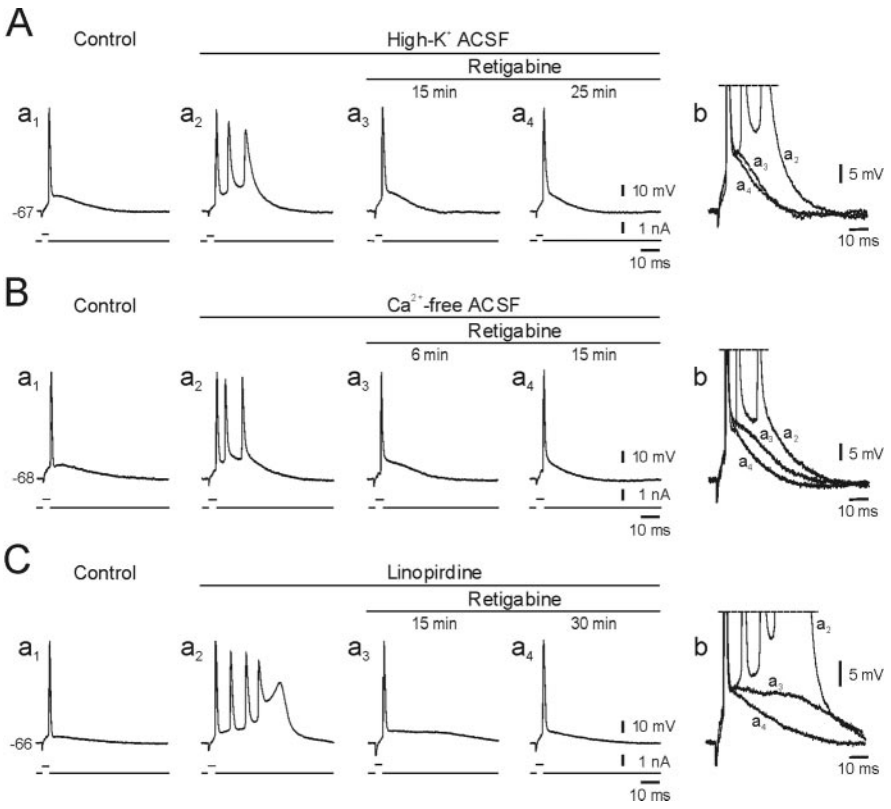

Figure 7. Retigabine suppresses intrinsic bursting in CA1 pyramidal cells. *A*, The effects of retigabine on intrinsic bursting induced by elevating K^+ concentration in the ACSF to 7.5 mM. In normal ACSF, the neuron fired a solitary spike in response brief stimuli (a_1). Changing to high-K^+ ACSF converted it to burst mode (a_2). Adding 10 μM retigabine to the latter ACSF suppressed the burst response by decreasing the underlying spike ADP (a_3, a_4). Portions of the traces in a_2–a_4 are expanded and overlaid in *b*. *B*, The effects of retigabine on intrinsic bursting induced by Ca^{2+}-free ACSF. In normal ACSF, the neuron fired a solitary spike in response brief stimuli (a_1). Changing to Ca^{2+}-free ACSF converted it to the burst mode (a_2). Adding 10 μM retigabine to the latter ACSF suppressed the burst response by decreasing the underlying spike ADP (a_3, a_4). Portions of the traces in a_2–a_4 are expanded and overlaid in *b*. *C*, The effects of retigabine on intrinsic bursting induced by linopirdine. In normal ACSF, the neuron fired a solitary spike in response to brief stimuli (a_1). Exposure to 10 μM linopirdine converted it to the burst mode (a_2). Adding 10 μM retigabine to the linopirdine-containing ACSF suppressed the burst response by decreasing the underlying spike ADP (a_3, a_4). Portions of the traces in a_2–a_4 are expanded and overlaid in *b*.

The facilitation of the spike ADP by linopirdine decreased with hyperpolarization of the neuron. Hyperpolarizing the neuron not only prevents I_{NaP} activation after the spike but also reduces the input resistance of the neuron by activating a cationic conductance (responsible for I_H) (Halliwell and Adams, 1982; Maccaferri et al., 1993), thereby reducing the depolarizing efficacy of residual I_{NaP}. Furthermore, because of the differential voltage sensitivity of I_H and I_M, depolarizing perturbations at hyperpolarized potentials are counteracted by deactivation of I_H, rather than by activation of I_M (Hu et al., 2002). It is, therefore, possible that at hyperpolarized potentials the spike ADP is abated by I_H, rather than by I_M, and therefore will not be affected by inhibiting I_M.

Blocking I_M facilitated the subthreshold ADPs in the same way it facilitated the spike ADPs, whereas augmenting I_M exerted the opposite effect. These data indicate that I_M is the major outward current damping these potentials. Thus, the ratio I_{NaP}/I_M determines the subthreshold electrical behavior of these neurons not only immediately after a spike but also in between spikes. Because the natural counterparts of subthreshold ADPs are EPSPs, it is expected that the EPSP waveform will also be modulated by I_{NaP} and I_M. Indeed, it has been shown in CA1 pyramidal cells that subthreshold EPSPs are boosted by somatic I_{NaP} (Andreasen and Lambert, 1999), whereas in another study we found that I_M curtails the EPSPs (Y. Yue and Y. Yaari, unpublished observations).

Additional effects of KCNQ/M channel blockers

Both linopirdine and XE991 mildly attenuated the fast repolarization of the spike, particularly its late component. It is unlikely that this effect is attributable to block of KCNQ/M channels that are active at rest or open during the spike. First, linopirdine also attenuated fast spike repolarization at hyperpolarized potentials, at which all KCNQ/M channels are deactivated. Second, KCNQ/M channels are too slow to activate during the fast spike and, therefore, cannot contribute substantially to its repolarization. Third, retigabine reversed the linopirdine-induced ADP facilitation but not its effects on spike repolarization. It is more likely that linopirdine attenuates spike repolarization by reducing I_C (10 μM linopirdine blocks ~40% of I_C) (Schnee and Brown, 1998). Our finding that this effect is occluded, rather than enhanced, by prior block of I_C with paxilline or iberiotoxin is congruent with this conclusion. A similar explanation may also apply to XE991, but its effects on K^+ channels other than KCNQ channels have not been scrutinized in hippocampal neurons.

Comparison with previous studies

The functional role of KCNQ/M channels has been studied previously in a variety of neurons, mostly using muscarinic receptor stimulation to inhibit I_M. However, the interpretation of these experiments is constrained by the fact that muscarinic stimulation exerts multiple effects on membrane ion channels (Caulfield et al., 1993). Indeed, some of these effects, such as depression of I_{NaP} (Mittmann and Alzheimer, 1998) or enhancement of the delayed rectifier K^+ current (I_K) (Zhang et al., 1992), lead to suppression of spike ADPs and associated bursting in CA1 pyramidal cells (Azouz et al., 1994; Alroy et al., 1999).

Although the data presented here unequivocally show that blocking I_M facilitates the spike ADP and induces bursting in CA1 pyramidal cells, a previous study proclaimed that 10 μM linopirdine has no effect on the spike ADP (Aiken et al., 1995). However, the latter study was conducted at low temperature (23°C), which may reduce the capacity of the neurons to generate an active ADP and spike bursts.

Exposing CA1 pyramidal cells to millimolar concentrations of 4-AP to block fast inactivating K^+ channels also facilitates the somatic spike ADP and induces bursting (Magee and Carruth, 1999). These effects have been attributed to enhanced invasion of apical dendrites by the backpropagating spike because of suppression of the fast inactivating K^+ current (I_A), leading to a local Ca^{2+} spike that reinforces the somatic spike ADP. Because apical

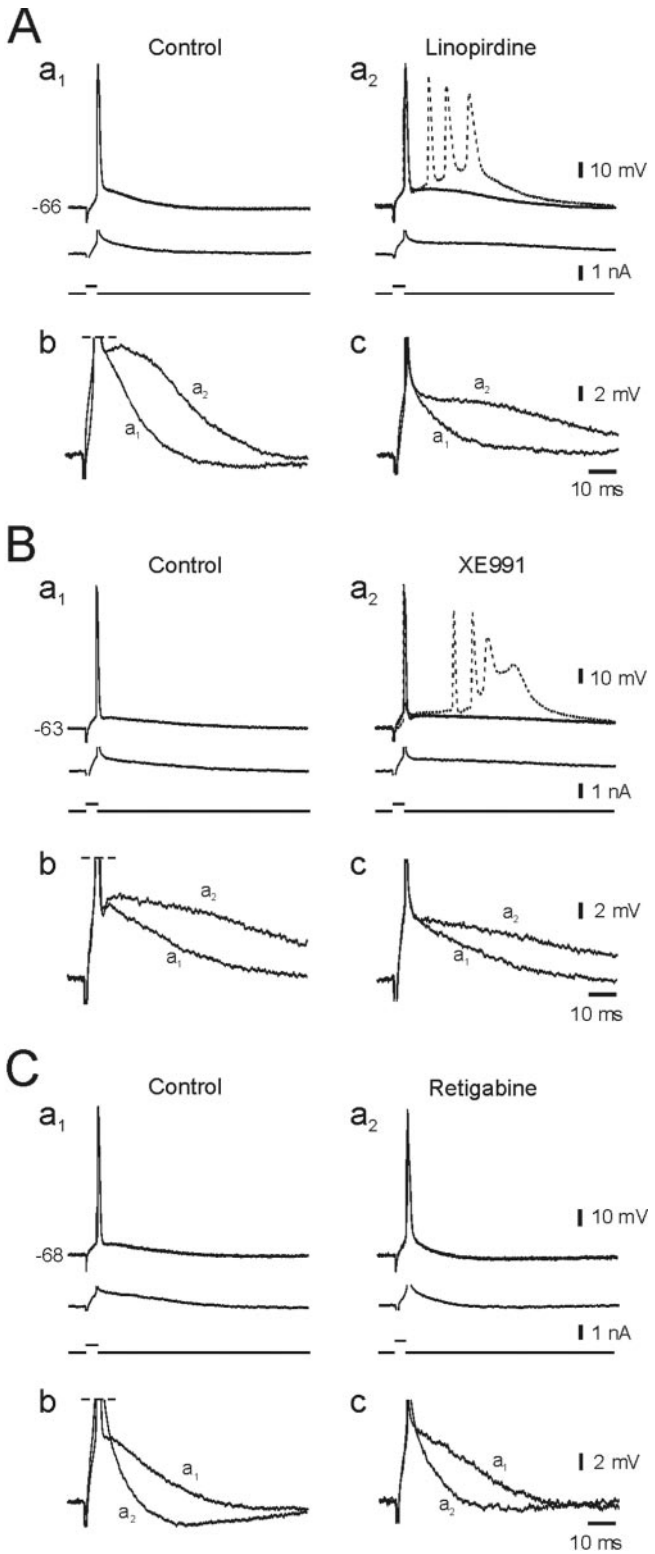

Figure 8. Effects of linopirdine, XE991, and retigabine on subthreshold ADPs. *A*, Effects of linopirdine. The neuron was stimulated with brief (4 msec) threshold-straddling depolarizing current pulses that evoked spikes in approximately half of the trials (a_1, top trace) and subthreshold responses in the other trials (a_1, middle trace). Adding 10 μM linopirdine to the ACSF facilitated the spike ADP (a_2, top solid trace) until it elicited a burst (a_2, top dashed trace) and also facilitated the subthreshold ADP (a_2, middle trace). Portions of the top traces in a_1 and a_2 are expanded and overlaid in *b* to facilitate comparison of spike ADPs. Likewise, portions of the middle traces in a_1 and a_2 are expanded and overlaid in *c* to facilitate comparison of subthreshold ADPs. *B*, Effects of XE991. This neuron was also stimulated with brief (4 msec) threshold-straddling depolarizing current pulses that evoked spikes in approximately half of the trials (a_1, top trace) and subthreshold responses in the other trials (a_1, middle trace). Adding 3 μM XE991 to the ACSF facilitated the spike ADP (a_2, top solid trace) until it elicited a burst (a_2, top dashed trace) and also facilitated the subthreshold ADP (a_2, middle trace). Portions of the top traces in a_1 and a_2 are expanded and overlaid in *b* to facilitate comparison of spike ADPs. Likewise, portions of the middle traces in a_1 and a_2 are expanded and overlaid in *c* to facilitate comparison of subthreshold ADPs. *C*, Effects of retigabine. This neuron also was stimulated with brief (4 msec) threshold-straddling depolarizing current pulses that evoked spikes in approximately half of the trials (a_1, top trace) and subthreshold responses in the other trials (a_1, middle trace). Adding 10 μM retigabine to the ACSF suppressed the spike ADP (a_2, top trace) and the subthreshold ADP (a_2, middle trace). Portions of the top traces in a_1 and a_2 are expanded and overlaid in *b* to facilitate comparison of spike ADPs. Likewise, portions of the middle traces in a_1 and a_2 are expanded and overlaid in *c* to facilitate comparison of subthreshold ADPs.

dendrites of CA1 pyramidal cells express KCNQ channels (Shah et al., 2002), a similar mechanism may contribute to spike ADP facilitation by linopirdine and XE991. This, however, is not likely, because linopirdine facilitated the spike ADP and also induced bursting in neurons lacking most of their apical dendrites or in neurons perfused with Ca^{2+}-free ACSF (Yue and Yaari, unpublished observations). Thus, it seems that I_M and I_A ordinarily prevent the escalation of the spike ADP into a spike burst in two distinct but complementary ways: (1) I_M counteracts the depolarizing action of I_{NaP} at the soma; and (2) I_A counteracts the depolarizing action of Ca^{2+} currents at the apical dendrites.

Functional implications

Here, we show for the first time that KCNQ/M channels critically control the intrinsic firing pattern of principal hippocampal neurons. Activation of these channels during the spike ADP normally prevents its escalation into a spike burst. When this activation is compromised, the propensity to generate spike bursts increases. Clearly, such a change in the input–output relationship of the neurons would markedly modify the operation of the neuronal network, because the downstream effect of a burst is much stronger than that of a solitary spike (Miles and Wong, 1987; Lisman, 1997; Kepecs and Lisman, 2003).

Hippocampal pyramidal cells *in vivo* were shown to alternate between regular firing ("simple" spikes) and burst firing ("complex" spikes), depending on the behavioral state of the animal (Ranck, 1973). It is not yet known how intrinsic factors contribute to complex spike bursting *in vivo*. However, with respect to the number and frequency domain of intraburst spikes, complex spikes in CA1 pyramidal cells (Harris et al., 2001) are remarkably similar to intrinsic bursts recorded *in vitro* after blocking KCNQ/M channels. It is possible, therefore, that transitions from simple to complex spiking and vice versa involve modulation of KCNQ/M channels. Multiple hippocampal neurotransmitters were shown to down- or up-modulate these channels (Brown and Yu, 2000). The release of these modulators *in vivo* may associate different behavioral states with different intrinsic firing patterns of CA1 pyramidal cells. Such associations may have functional significance. For example, the incidence of complex spikes increases when rats are subjected to learning paradigms (Otto et al., 1991), and several studies have shown that postsynaptic bursting greatly enhances long-term synaptic plasticity (Thomas et al., 1998; Pike et al., 1999). Thus, neurotransmitter modulation of KCNQ/M channels *in vivo* may regulate synaptic plasticity and hence learning and memory, via its effects on intrinsic neuronal firing patterns. Interestingly, KCNQ channel blockers improve performance of cognitively impaired rodents in several tests of learning and memory (Fontana et al., 1994). It is tempting to

speculate that these drugs enhance cognition by induction of complex spiking subsequent to the block of KCNQ/M channels.

Finally, our findings may be pertinent to the mechanism of inherited neonatal epilepsy that recently has been linked to loss-of-function mutations in KCNQ2 and KCNQ3 (Jentsch, 2000). Because down-modulation of KCNQ/M channels induces intrinsic bursting, it is very likely that KCNQ/M channel-mutated neurons are more prone to fire in the burst mode than their normal counterparts. A large body of evidence suggests that intrinsically bursting neurons play a key role in triggering epileptiform discharges when GABAergic synaptic inhibition is compromised (Yaari and Beck, 2002). Given that GABAergic synapses are excitatory in early life (Cherubini et al., 1991), such bursting activity may easily spread in the neonatal brain, leading to abnormal synchronization of repetitive discharge that underlies epileptic seizures.

References

Aiken SP, Lampe BJ, Murphy PA, Brown BS (1995) Reduction of spike frequency adaptation and blockade of M-current in rat CA1 pyramidal neurones by linopirdine (DuP 996), a neurotransmitter release enhancer. Br J Pharmacol 11:1163–1168.

Alroy G, Su H, Yaari Y (1999) Protein kinase C mediates muscarinic block of intrinsic bursting in rat hippocampal neurons. J Physiol (Lond) 518:71–79.

Andreasen M, Lambert JDC (1999) Somatic amplification of distally generated subthreshold EPSPs in rat hippocampal pyramidal neurones. J Physiol (Lond) 519:85–100.

Azouz R, Jensen AM, Yaari Y (1994) Muscarinic modulation of intrinsic burst firing in rat hippocampal neurons. Eur J Neurosci 6:961–966.

Azouz R, Jensen MS, Yaari Y (1996) Ionic basis of spike afterdepolarization and burst generation in adult rat hippocampal CA1 pyramidal cells. J Physiol (Lond) 492:211–223.

Brown BS, Yu SP (2000) Modulation and genetic identification of the M channel. Prog Biophys Mol Biol 73:135–166.

Brown DA (1988) M currents. In: Ion channels, Vol 1 (Narahashi T, ed), pp 55–99. New York: Plenum.

Brown DA, Adams PR (1980) Muscarinic suppression of a novel voltage-sensitive K^+ current in a vertebrate neurone. Nature 283:673–676.

Caulfield MP, Robbins J, Higashida H, Brown DA (1993) Postsynaptic actions of acetylcholine: the coupling of muscarinic receptor subtypes to neuronal ion channels. Prog Brain Res 98:293–301.

Cherubini E, Gaiarsa JL, Ben Ari Y (1991) GABA: an excitatory transmitter in early postnatal life. Trends Neurosci 14:515–519.

Cole AE, Nicoll RA (1983) Acetylcholine mediates a slow synaptic potential in hippocampal pyramidal cells. Science 221:1299–1301.

Dreixler JC, Bian J, Cao Y, Roberts MT, Roizen JD, Houamed KM (2000) Block of rat brain recombinant SK channels by tricyclic antidepressants and related compounds. Eur J Pharmacol 401:1–7.

Fontana DJ, Inouye GT, Johnson RM (1994) Linopirdine (DuP 996) improves performance in several tests of learning and memory by modulation of cholinergic neurotransmission. Pharmacol Biochem Behav 49:1075–1082.

French CR, Sah P, Buckett KJ, Gage PW (1990) A voltage-dependent persistent sodium current in mammalian hippocampal neurons. J Gen Physiol 95:1139–1157.

Halliwell JV, Adams PR (1982) Voltage-clamp analysis of muscarinic excitation in hippocampal neurons. Brain Res 250:71–92.

Harris KD, Hirase H, Leinekugel X, Henze DA, Buzsaki G (2001) Temporal interaction between single spikes and complex spike bursts in hippocampal pyramidal cells. Neuron 32:141–149.

Hu H, Vervaeke K, Storm JF (2002) Two forms of electrical resonance at theta frequencies, generated by M-current, h-current and persistent Na^+ current in rat hippocampal pyramidal cells. J Physiol (Lond) 545:783–805.

Jensen MS, Azouz R, Yaari Y (1994) Variant firing patterns in rat hippocampal pyramidal cells modulated by extracellular potassium. J Neurophysiol 71:831–839.

Jensen MS, Azouz R, Yaari Y (1996) Spike after-depolarization and burst generation in adult rat hippocampal CA1 pyramidal cells. J Physiol (Lond) 492:199–210.

Jentsch TJ (2000) Neuronal KCNQ potassium channels: physiology and role in disease. Nat Rev Neurosci 1:21–30.

Kepecs A, Lisman J (2003) Information encoding and computation with spikes and bursts. Network 14:103–118.

Khawaled R, Bruening-Wright A, Adelman JP, Maylie J (1999) Bicuculline block of small-conductance calcium-activated potassium channels. Pflügers Arch 438:314–321.

Lancaster B, Nicoll RA (1987) Properties of two calcium-activated hyperpolarizations in rat hippocampal neurones. J Physiol (Lond) 389:187–203.

Lisman JE (1997) Bursts as a unit of neural information: making unreliable synapses reliable. Trends Neurosci 20:38–43.

Maccaferri G, Mangoni M, Lazzari A, DiFrancesco D (1993) Properties of the hyperpolarization-activated current in rat hippocampal CA1 pyramidal cells. J Neurophysiol 69:2129–2136.

Madison DV, Nicoll RA (1984) Control of repetitive discharge of rat CA1 pyramidal neurones in vitro. J Physiol (Lond) 354:319–331.

Magee JC, Carruth M (1999) Dendritic voltage-gated ion channels regulate the action potential firing mode of hippocampal CA1 pyramidal neurons. J Neurophysiol 82:1895–1901.

Main MJ, Cryan JE, Dupere JR, Cox B, Clare JJ, Burbidge SA (2000) Modulation of KCNQ2/3 potassium channels by the novel anticonvulsant retigabine. Mol Pharmacol 58:253–262.

McCormick DA, Wang Z, Huguenard J (1993) Neurotransmitter control of neocortical neuronal activity and excitability. Cereb Cortex 3:387–398.

Miles R, Wong RK (1987) Inhibitory control of local excitatory circuits in the guinea-pig hippocampus. J Physiol (Lond) 388:611–629.

Mittmann T, Alzheimer C (1998) Muscarinic inhibition of persistent $Na+$ current in rat neocortical pyramidal neurons. J Neurophysiol 79:1579–1582.

Otto T, Eichenbaum H, Wiener SI, Wible CG (1991) Learning-related patterns of CA1 spike trains parallel stimulation parameters optimal for inducing hippocampal long-term potentiation. Hippocampus 1:181–192.

Passmore GM, Selyanko AA, Mistry M, Al-Qatari M, Marsh SJ, Matthews EA, Dickenson AH, Brown TA, Burbidge SA, Main M, Brown DA (2003) KCNQ/M currents in sensory neurons: significance for pain therapy. J Neurosci 23:7227–7236.

Pike FG, Meredith RM, Olding AW, Paulsen O (1999) Rapid report: postsynaptic bursting is essential for "Hebbian" induction of associative long-term potentiation at excitatory synapses in rat hippocampus. J Physiol (Lond) 518:571–576.

Ranck Jr JB (1973) Studies on single neurons in dorsal hippocampal formation and septum in unrestrained rats. I. Behavioral correlates and firing repertoires. Exp Neurol 41:461–531.

Rundfeldt C, Netzer R (2000) The novel anticonvulsant retigabine activates M-currents in Chinese hamster ovary-cells transfected with human KCNQ2/3 subunits. Neurosci Lett 282:73–76.

Schnee ME, Brown BS (1998) Selectivity of linopirdine (DuP 996), a neurotransmitter release enhancer, in blocking voltage-dependent and calcium-activated potassium currents in hippocampal neurons. J Pharmacol Exp Ther 286:709–717.

Schroeder BC, Hechenberger M, Weinreich F, Kubisch C, Jentsch TJ (2000) KCNQ5, a novel potassium channel broadly expressed in brain, mediates M-type currents. J Biol Chem 275:24089–24095.

Schwartzkroin PA (1975) Characteristics of CA1 neurons recorded intracellularly in the hippocampal in vitro slice preparation. Brain Res 85:423–436.

Schweitzer P (2000) Cannabinoids decrease the K^+ M-current in hippocampal CA1 neurons. J Neurosci 20:51–58.

Shah M, Mistry M, Marsh SJ, Brown DA, Delmas P (2002) Molecular correlates of the M-current in cultured rat hippocampal neurons. J Physiol (Lond) 544:29–37.

Shao LR, Halvorsrud R, Borg-Graham L, Storm JF (1999) The role of BK-type Ca^{2+}-dependent K^+ channels in spike broadening during repetitive firing in rat hippocampal pyramidal cells. J Physiol (Lond) 521:135–146.

Stocker M, Krause M, Pedarzani P (1999) An apamin-sensitive Ca^{2+}-activated K^+ current in hippocampal pyramidal neurons. Proc Natl Acad Sci USA 96:4662–4667.

Storm JF (1987) Action potential repolarization and a fast after-hyperpolarization in rat hippocampal pyramidal cells. J Physiol (Lond) 385:733–759.

Storm JF (1988) Temporal integration by a slowly inactivating K^+ current in hippocampal neurons. Nature 336:379–381.

Storm JF (1989) An after-hyperpolarization of medium duration in rat hippocampal pyramidal cells. J Physiol (Lond) 409:171–190.

Su H, Alroy G, Kirson ED, Yaari Y (2001) Extracellular calcium modulates persistent sodium current-dependent intrinsic bursting in rat hippocampal neurons. J Neurosci 27:4173–4182.

Tatulian L, Delmas P, Abogadie FC, Brown DA (2001) Activation of expressed KCNQ potassium currents and native neuronal M- type potassium currents by the anticonvulsant drug retigabine. J Neurosci 21:5535–5545.

Thomas MJ, Watabe AM, Moody TD, Makhinson M, O'Dell TJ (1998) Postsynaptic complex spike bursting enables the induction of LTP by theta frequency synaptic stimulation. J Neurosci 18:7118–7126.

Wang HS, Pan Z, Shi W, Brown BS, Wymore RS, Cohen IS, Dixon JE, McKinnon D (1998) KCNQ2 and KCNQ3 potassium channel subunits: molecular correlates of the M-channel. Science 282:1890–1893.

Wickenden AD, Yu W, Zou A, Jegla T, Wagoner PK (2000) Retigabine, a novel anti-convulsant, enhances activation of KCNQ2/Q3 potassium channels. Mol Pharmacol 58:591–600.

Yaari Y, Beck H (2002) "Epileptic Neurons" in temporal lobe epilepsy. Brain Pathol 12:234–239.

Zhang L, Weiner JL, Carlen PL (1992) Muscarinic potentiation of I_K in hippocampal neurons: electrophysiological characterization of the signal transduction pathway. J Neurosci 12:4510–4520.